Numerical simulation and field synergy analysis of heat transfer performance of radial slit fin surface

Jun-Jie Zhou, Zhi-Gen Wu and Wen-Quan Tao*

School of Energy and Power Engineering,
State Key Laboratory of Multiphase Flow in Power Engineering,
Xi'an Jiaotong University, Shananxi, Xi'an 710049, China
E-mail: Zhoujj@zzu.edu.cn E-mail: wuzhigen@mailst.xjtu.edu.cn
E-mail: wqtao@mail.xjtu.edu.cn
*Corresponding author

Abstract: The finite volume method is used to numerically simulate the laminar heat transfer performances of a plate fin-and-tube heat exchanger surface with radially positioned slots and a plain plate fin-and-tube surface. It is found that at the identical pumping power or identical pressure drop, the performance of the slotted fin surface is much better than that of the plain fin surface, while under the identical mass flow rate, the performance of the slotted fin is inferior to that of the plain one, and where there is an enhanced heat transfer, there is a better synergy between velocity and temperature gradient.

Keywords: numerical simulation; field synergy principle; plain plate fin; radial slit fin; heat transfer performance; identical pumping power; identical pressure drop; identical mass flow rate.

Reference to this paper should be made as follows: Zhou, J-J., Wu, Z-G. and Tao, W-Q. (2006) 'Numerical simulation and field synergy analysis of heat transfer performance of radial slit fin surface', *Progress in Computational Fluid Dynamics*, Vol. 6, No. 7, pp.419–427.

Biographical notes: Jun-Jie Zhou is currently a Lecturer at the School of Chemical Engineering of Zheng Zhou University, China. He received his Bachelor of Civil Engineering in 1998 and his Master of Safety Technology and Engineering in 2001 from Xi'an Science and Technology University. He received PhD in Engineering Thermophsics from Xi'an Jiaotong University in 2005. He has published more than 10 technical articles in both numerical simulation and heat transfer. His research interests include numerical heat transfer, heat transfer enhancement, energy saving and CAE analysis.

Zhi-Gen Wu is currently a Doctoral graduate student at the School of Energy and Power Engineering of Xi'an Jiaotong University, China (XJTU). He received his Bachelor of engineering in Mechanical Engineering in 2002 from XJTU. His research interests include numerical simulation and experimental study of fin-and-tube heat exchangers, and CO2 transcritical air condition system.

W.Q. Tao is a Professor of Engineering Thermophysics at the Xi'an Jiaotong University, China. He graduated from Xi'an Jiaotong University in 1962, and received his graduate diploma in 1966. He has published over 300 papers. He is also the author or co-author of nine textbooks. He is now the member of advisory board of Numerical Heat Transfer, member of Editorial Board of *Progress in Computational Fluid Dynamics*, the Associate Editor of *International Journal of Heat Mass Transfer*, and *Communication in Heat Mass Transfer*. His research interests include advanced computational heat transfer, heat transfer enhancement, micro and mini channel heat transfer, cooling techniques of electronics.

1 Introduction

Finned-tube heat exchangers have been widely used in air-conditioning, refrigeration, chemistry and power industries. With increasing requirement for high efficient, compact, lightweight and reliable gas/liquid heat exchangers, it is becoming important that enhanced heat transfer of plate fin-and-tube heat exchanger is researched. Various types of interrupted surfaces are proposed for the enhancement of gas-side heat transfer, including the wavy or corrugated fin, offset strip fin and louver fin, etc. A lot of experimental and/or numerical studies have been conducted on airside heat transfer performance. For the simplicity of presentation, only some recent related references are reviewed in the following section.

Min and Webb (2001) studied the plate fin-and-tube heat exchanger with wavy surface by FLUENT to predict the airside heat transfer and flow friction characteristics. Leu et al. (2001) conducted a numerical simulation of airside performance of louvered fin-and-tube heat exchanger

having circular and oval configurations by PHOENICS. Atkinson et al. (1998) compared two- and three-dimensional numerical models of flow and heat transfer over louvered fin arrays in compact heat exchangers by START-CD. They concluded that 3-D models could give more accurate prediction of overall heat transfer than 2-D models. Using a finite-element discretisation method, Comini and Croce (2001) studied the flow and heat transfer in the flow passages of the tube fin exchangers with wavy, offset-strip, and louver fin surfaces by using a simplified two-dimensional model without tube. Cheng et al. (2004) and Qu et al. (2004) studied heat transfer and pressure drop performance for the X-arrangement of strips. Yun and Lee (2000) studied influence of design parameters on the heat transfer and flow friction characteristics of the heat exchanger with slit fins.

In most of the above referenced papers, major concerns are focused on the geometric factors, which affect heat transfer coefficient and friction factor by experimental measurements or numerical computations. Very few papers paid enough attention on the basic mechanism of heat transfer enhancement in such plate fin-and-tube heat exchangers. It is very essential to study the basic enhancement mechanism, because such basic mechanism not only deepens our understanding of convective heat transfer process, but also serves as guide in the further development of new type enhanced surface.

Guo et al. (1998) proposed a new concept of enhancing convective heat transfer. By integrating the boundary layer energy equation along the boundary thickness, they concluded that by decreasing the angle between fluid velocity and its temperature gradient, the heat transfer could be enhanced. Later this concept was shown also applicable to the elliptic flow (Tao et al., 2002a), and the existing three explanations for the enhanced convective heat transfer can be unified by this concept (Tao et al., 2002b). This new concept is now named as field synergy principle (FSP).

With air-conditioning heat transfer surface as background, the present study provides the numerical solutions for the plain plate fin and slotted fin heat transfer surface of two-row tube in staggered arrangement with fixed fin pitch (1.2 mm) under different values of inlet frontal velocity. The complex flow structure and local heat transfer characteristics are revealed in detail. Focus is concentrated on the heat transfer enhancement mechanism, and the FSP is adapted to analyse the numerical results. Comparisons of performance are made for the two types of fin surfaces based on three constraints.

2 Mathematic models and solution method

2.1 Physical models

A schematic diagram of a two-row plate fin-and-tube heat exchanger is presented in Figure 1. The physical problem to be studied can be described as follows: warm air flows along the fin surfaces and the cooling water goes through inside the tubes. The heat is transmitted from the air to the tube wall and the fin surface, and then to the cooling water. The tube and fin are made of copper and aluminium, respectively. The heat transfer and pressure drop characteristics of the airsides are to be solved by numerical modelling.

Figure 1 Schematic diagram of a two-row plate fin-and-tube heat exchanger

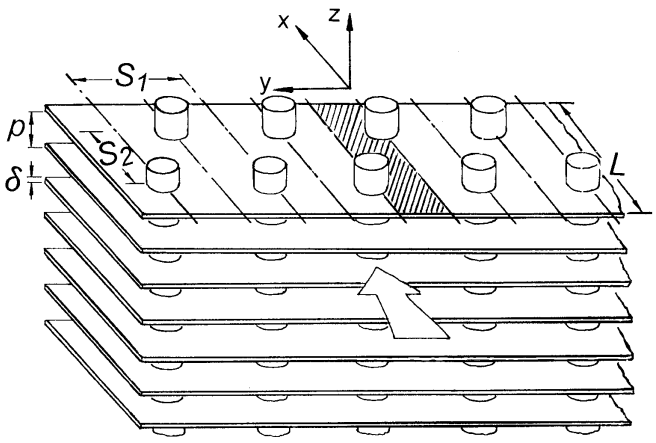

Now the computational domain is considered. From the periodicity and symmetric condition of tube arrangement, the fluid flow and heat transfer characteristics in the shaded area shown in Figure 1 between two adjacent fin sheets can be regarded as being representative of the entire heat exchanger. The computational domain for such selected unit is presented in Figure 2. The slotted fin surface studied in this paper has strips arranged radially, and the inclined boundaries of the strips are simulated by stepwise approximation. The corresponding plain plate fin surface is shown in Figure 3. In the actual simulation, for the use of uniform inlet velocity condition, an extended upstream region of 1.5 times fin length is added before the fin sheet, while for the usage of local one-way assumption, an after region of 5 times fin length is patched after the fin surface. A pictorial view of such extended full computational domain is provided in Figure 4. Because of the space limitation, the pre-fin and after-fin region lengths in the figure are not in scale. The cross-section view of the computational domain is presented in Figure 5. As seen there, the computational region is within the two symmetric planes going through the two adjacent fin sheets, of which, half thickness of the two fin sheets are the top and bottom parts. The strips are protruded alternatively up and down along the flow direction, which are not shown in the figure for simplicity. The dashed lines in Figures 4 and 5 present the extended region mentioned above. Thus the simulated structure is rather complicated, and the temperature distributions both in the fin sheets and in the fluid must be simultaneously computed, making the problem being of conjugated type (Patankar, 1980).

Figure 2 Computational domain of the fin region

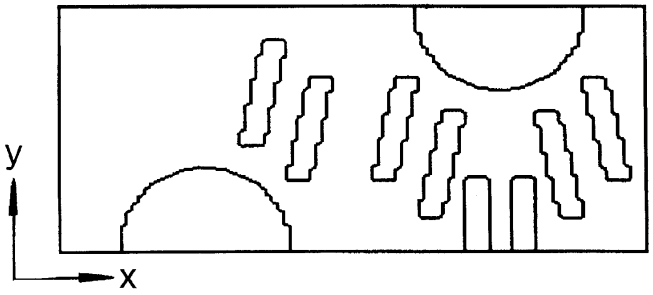

Figure 3 Dimension of plain plate fin

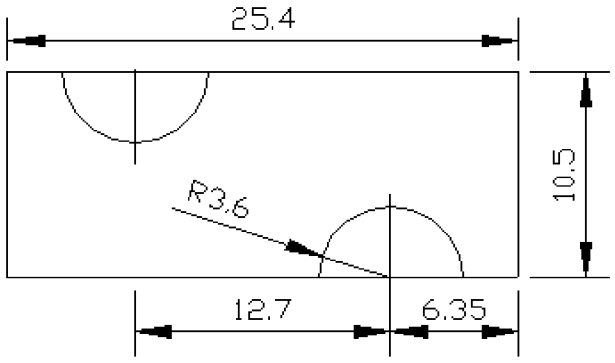

Figure 4 Pictorial view of the full computational domain

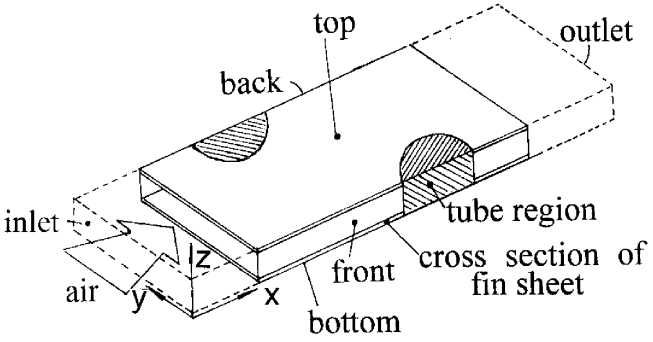

Figure 5 Cross-section view of the full computational domain

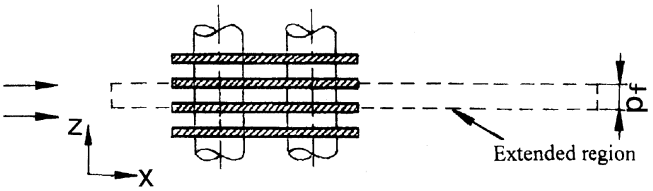

Jacobi and Shah (1998) pointed out that the flow is strongly affected by the interrupted surface geometry, at low Reynolds number based on hydraulic diameter (less than 400), flow through offset-strip geometry is laminar and nearly steady. For intermediate Reynolds numbers (roughly $400 < Re_{Dh} < 1000$), the flow remains laminar, but unsteadiness and vortex shedding become important. For the present front velocity range from 1.0 m/s to 3.0 m/s, corresponding Reynolds number based on hydraulic diameter is roughly from 150 to 450. Therefore a steady model was used in our study. Furthermore, the major focus of the present study is for the average heat transfer performance of the new type slotted fin surface. According to the numerical study in He et al. (2005), the average heat transfer performance obtained by using steady model and transfer model for plate fin surfaces give almost the same results, with a difference being in the order of 1%.

The following assumptions are adopted in the numerical modelling:

- the contact thermal resistance between the tube and the fin sheet is neglected
- because of the relatively high heat transfer coefficient between the cooling water and the inner wall of the tube, and the high thermal conductivity of the tube wall, the tube wall is assumed to be at constant temperature
- the thermophysical properties of both the fluid and the tube-fin set are constant
- the flow is laminar, incompressible and in steady state.

Numerical simulations are conducted with an approaching velocity ranging from 1.0 m/s to 3.0 m/s. The configuration geometries are shown in Figure 3. The round tube diameter equals 7.2 mm, and the longitudinal tube pitch is 12.7 mm. The fin thickness is 0.105 mm.

2.2 Mathematical formulation

2.2.1 Governing equations

According to the above physical model, following governing equations can be obtained.

Mass conservation equation is:

$$\frac{\partial(\rho u)}{\partial x}+\frac{\partial(\rho v)}{\partial y}+\frac{\partial(\rho \omega)}{\partial z}=0. \tag{1}$$

The conservation equations for momentum and energy can be written in a general form as follows:

$$\begin{aligned}&\frac{\partial(\rho u\phi)}{\partial x}+\frac{\partial(\rho v\phi)}{\partial y}+\frac{\partial(\rho \omega\phi)}{\partial z}\\&=\frac{\partial}{\partial x}\left(\Gamma_\phi\frac{\partial\phi}{\partial x}\right)+\frac{\partial}{\partial y}\left(\Gamma_\phi\frac{\partial\phi}{\partial y}\right)+\frac{\partial}{\partial z}\left(\Gamma_\phi\frac{\partial\phi}{\partial z}\right)+S_\phi\end{aligned} \tag{2}$$

where ϕ is a general variable, Γ_ϕ is a nominal diffusion coefficient and S_ϕ is a general source term. Equation (2) is valid for both fluid and solid region, with the values of Γ_ϕ and S_ϕ being different.

2.2.2 Boundary conditions

In the specification of the boundary conditions, the pictorial view of the computational domain shown in Figure 4 will be referred.

- *Inlet boundary condition*: u = const, $v = w = 0$, T_{in} = const.
- *Outlet boundary condition*: the local one-way (Patankar, 1980) assumption is adopted.
- *Top and bottom boundary condition*: in the fin region, no slip condition is used for all velocities, and the symmetry boundary condition is applied for temperature, $\partial T/\partial z = 0$, the periodic boundary condition is applied to the fluid within the slots: $u(x,y,0) = u(x,y,p_f)$, $v(x,y,0) = v(x,y,p_f)$, $w(x,y,0) = w(x,y,p_f)$, $T(x,y,0) = T(x,y,p_f)$.
- *Front and back boundary condition*: the symmetry boundary condition is applied except for the tube and fin thickness region, $\partial u/\partial y = \partial v/\partial y = \partial T/\partial y = 0$, $v = 0$; in the tube region T_{tube} = const, $u = v = w = 0$; in the fin cross section region $u = v = w = 0$ and $\partial T/\partial y = 0$.

2.2.3 Grid system

For the convenience of code development, the three dimensional Cartesian coordinates are adopted. The domain extension method (Patankar, 1980) is applied to deal with the irregular boundaries and the tube-curved surface is simulated by the stepwise approximation. Preliminary computations with three grid systems, $136 \times 102 \times 14$, $136 \times 102 \times 24$ and $136 \times 102 \times 34$, were performed and the results are shown in Figure 6. Computation results reveal that the three tested grid systems have almost the same results for the average heat transfer and flow friction characteristics. Therefore, a grid system with $136 \times 102 \times 24$ grid nodes is used, which is enough fine for the present slit fin. The computational domain is meshed by non-uniform grids, with the grids in the fin coil region being fine, and that in the extension domain being coarse. The grid arrangements in the fin coil region are shown in Figure 7 for the slotted and plain plate fin surfaces, respectively.

Figure 6 Verification of grid independence

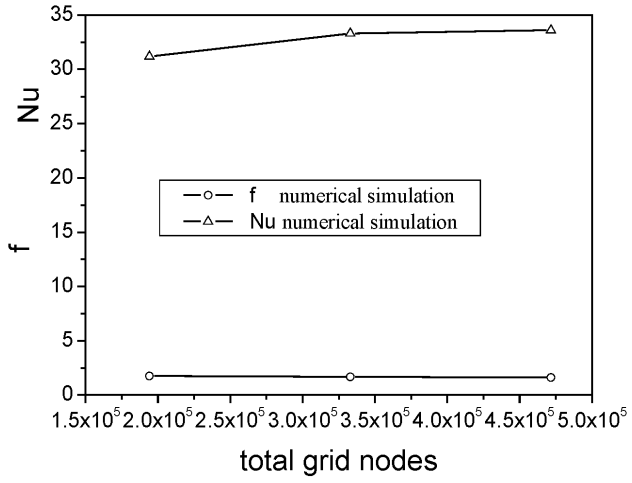

Figure 7 Computation grid system in the fin domain: (a) slotted fin and (b) plain plate fin

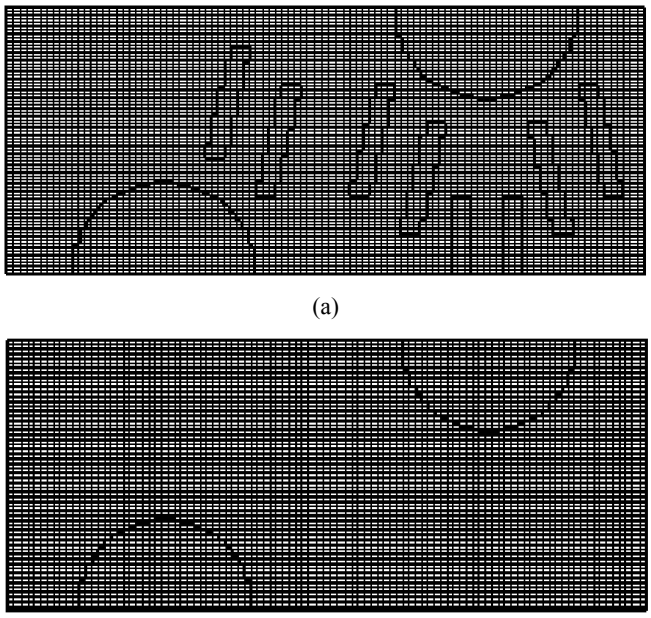

(a)

(b)

2.2.4 Numerical methods

The SIMPLE algorithm is used to deal with the linkage between velocity and pressure. Because of the non-linearity of the problem studied, under-relaxation in the solution process is applied. Solid region in the computational domain is treated as a special fluid with infinite viscosity. It is to be noted that in the governing Equation (2), the nominal diffusion coefficient for the temperature is $\Gamma = \lambda/c_p$, and the harmonic mean method is used to determine the interface diffusion coefficient. To guarantee that the heat flux rate of conjugated interface of fluid and solid is continuous, the thermal conductivity of solid and fluid are adopted from their actual values, respectively, while the heat capacity of solid is taken as that of the fluid (He et al., 2005).

3 Data reduction

The predicted overall pressure drop and heat transfer rate in the entire fin surface are determined by:

Pressure drop,

$$\Delta p = P_{out} - P_{in}. \tag{3}$$

Heat transfer rates,

$$Q = c_p m(T_{out} - T_{in}). \tag{4}$$

The overall friction factor, f, and the average Nusselt number, Nu, are calculated from the following equations,

$$f = -\frac{\Delta p}{(1/2)\rho V^2_{\max}} \tag{5}$$

$$\mathrm{Nu} = \frac{hd}{\lambda} \tag{6}$$

$$h = \frac{Q}{\Delta T_{\lg} A}. \tag{7}$$

The Reynolds number is determined by

$$\mathrm{Re} = \frac{V_{\max} d}{\nu}. \tag{8}$$

In the above definitions, d is the fin collar outside diameter of the tube, $d_o + 2\delta_f$, $V_{\max}$ is the average maximum fluid velocity at the minimum flow area within the tube banks, h is the average heat transfer coefficient of fin surface, A is the projection area in the x-y plane of the fin, $\Delta T_{\lg}$ is the logarithmic mean temperature difference between tube wall and the fluid.

The synergy angle, symbolised by θ, is the local intersection angle between velocity and temperature gradient and is calculated by:

$$\theta = \arccos\left(\frac{u(\partial T/\partial x) + v(\partial T/\partial y) + w(\partial T/\partial z)}{|\vec{U}||\mathrm{grad}T|}\right) \tag{9}$$

where u, v, w are the velocity components in x, y, and z directions, respectively.

The FSP indicates that the essence to enhance single-phase heat transfer is to reduce the intersection angle between the velocity and the temperature gradient. In this paper, the spanwise local averaged intersection angle is used as the symbol or indication of the spanwise synergy between the two fields. It is defined as follows:

$$\theta_x = \sum \frac{|\vec{u}| \bullet |\nabla T| \,\mathrm{d}A_i}{\sum |\vec{u}| \bullet |\nabla T| \,\mathrm{d}A_i} \bullet \theta_i \tag{10}$$

where $\mathrm{d}A_i$ is the area element of a control volume in the spanwise direction.

The local and average heat transfer coefficients, h_x and h, are defined as

$$h_x = \frac{q}{T_w - T_b}, \; h = \frac{Q}{A\Delta T_m} \tag{11}$$

where q is the local heat flux, T_b is the local bulk mean temperature of the fluid and Q is the total heat transfer rate of the fin surface. The local Nusselt number, $\mathrm{Nu_x}$, and the averaged Nusselt number, Nu, can be expressed as

$$\mathrm{Nu}_x = \frac{h_x}{\lambda} d, \; \mathrm{Nu} = \frac{h}{\lambda} d. \tag{12}$$

Performance comparisons between the plain plate fin and the slit fin will be conducted according to following criteria.

Based on identical mass flow rate,

$$\mathrm{NuF} = \frac{\mathrm{Nu}_{en}/\mathrm{Nu}_o}{f_{en}/f_o}. \tag{13}$$

Based on identical pressure drop,

$$\mathrm{NuF}_{1/2} = \frac{\mathrm{Nu}_{en}/\mathrm{Nu}_o}{(f_{en}/f_o)^{1/2}}. \tag{14}$$

Based on identical pumping power,

$$\mathrm{NuF}_{1/3} = \frac{\mathrm{Nu}_{en}/\mathrm{Nu}_o}{(f_{en}/f_o)^{1/3}} \tag{15}$$

where the subscript '0' refers to the plain plate fin (reference case) and 'en' stands for the enhanced design.

4 Results and discussion

4.1 Experimental validation

As a first step in the numerical investigation of the physical problem, we justify our computer code by comparing our numerical predictions with the test data available in the literature. Figure 8 shows the comparisons of the average Nusselt number and friction factors between the numerical and experimental results (Kang et al., 1994) for a three-row slotted fin surface with parallel strips. As seen in the figure, the numerical predictions of Nu and f are in good agreement with the experimental results.

Figure 8 A comparison study between experimental and computational data for the slit fin

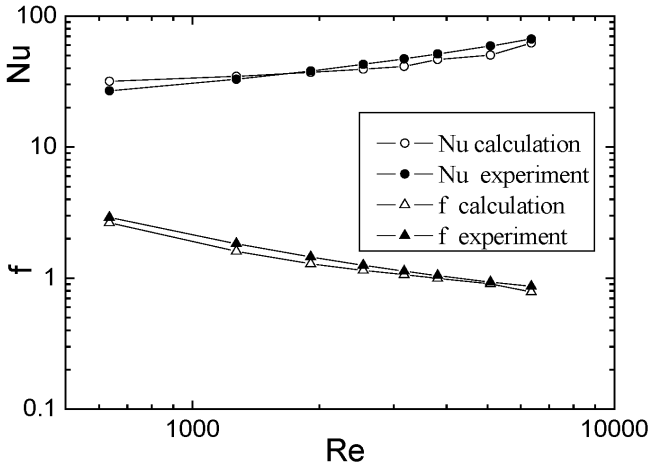

Source: Kang et al. (1994)

4.2 Overall performance comparison

The simulated heat transfer rate and pressure drop of the two types of fins in the frontal velocity of 1~3 m/s are presented in Figures 9 and 10. They reveal that both heat transfer rate and pressure drop of the two kinds of surfaces increase with the increase of the frontal velocity. At the same frontal velocity, the heat transfer rates of the slotted fin surface is higher than that of plain plate surface, and the pressure drop of the slotted fin is also higher than that of the plain one.

Figure 9 Q vs. V

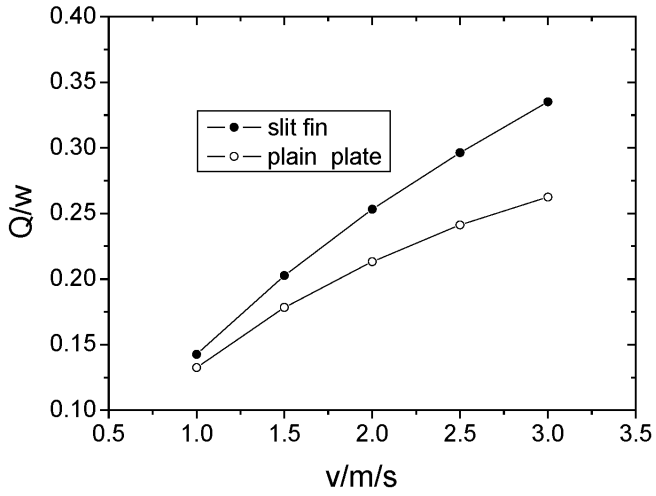

Figure 10 DP vs. V

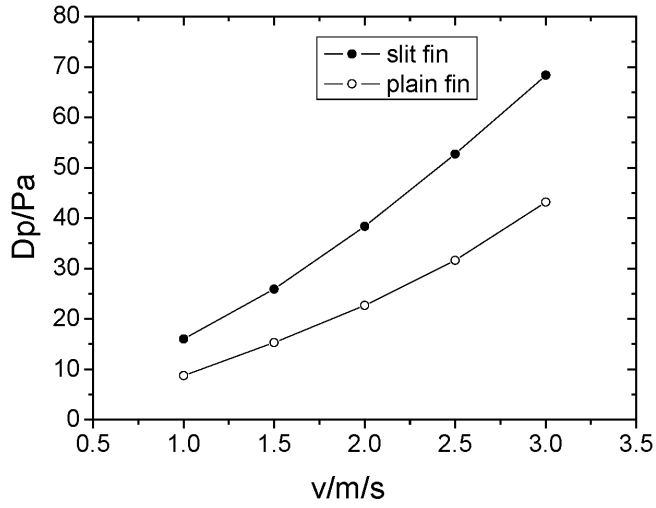

Figure 11 presents the variations of f and Nu vs. Re for the plain fin and slit fin. It reveals that both Nu and *f* of the two kinds of surfaces increase with the increase of Re. At the same Re, Nu and *f* of the slotted fin surface is higher than that of plain plate surface. The predicted Nusselt number and the friction factor of the slit fin and plain fin can be well correlated by power law equation in the range of Re from 700 to 2300 (i.e., the frontal velocity varies from 1.0 m/s to 3.0 m/s). They are

For slit fin

$$f = 240.2\,\mathrm{Re}^{-0.6758} \tag{16a}$$

$$\mathrm{Nu} = 9.9513\,\mathrm{Re}^{0.1653}. \tag{16b}$$

For plain plate fin

$$f = 63.53\,\mathrm{Re}^{-0.5646} \tag{17a}$$

$$\mathrm{Nu} = 8.905\,\mathrm{Re}^{0.1222}. \tag{17b}$$

Figure 11 Airside performance for the plain plate fin and slit fin

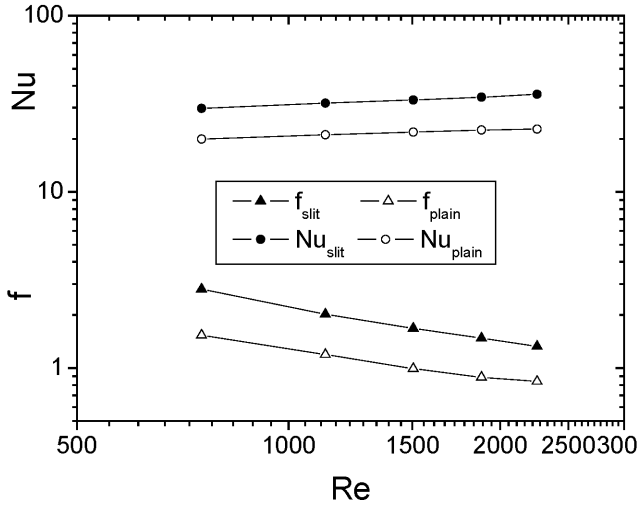

Figure 12 presents the comparison results based on the three criteria mentioned above. As can be seen there, NuF increases with the increase of Re, and the value of NuF is from 0.8 to 1.0. Webb (1994) points out that a very good enhanced fin may have a value of NuF of 0.8–0.9, but NuF is always less than 1.0. The same conclusion was also pointed out by Shah and Sekulic (2003). At the identical pressure drop and pumping power, however, $\mathrm{NuF}_{1/2}$ and $\mathrm{NuF}_{1/3}$ are larger than 1.0. For the case studied the range of $\mathrm{NuF}_{1/2}$ is from 1.1 to 1.3, and that of $\mathrm{NuF}_{1/3}$ is from 1.2 to 1.4. This implies that the performance of the slotted fin surface is much better than that of the plain fin surface under the identical pumping power constraint.

Figure 12 Comparison of airside performance for the plain plate fin and slit fin

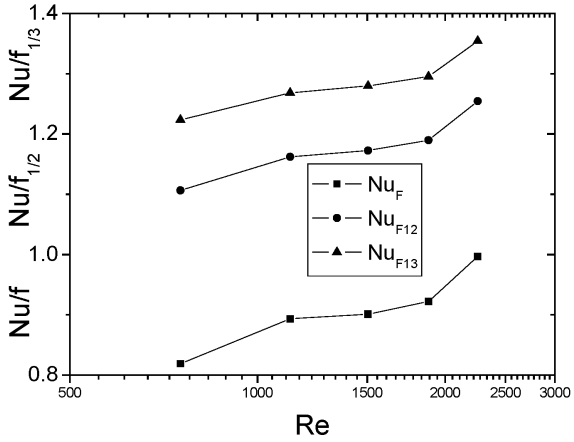

4.3 Local heat transfer characteristics

Figure 13 shows the variations of the spanwise averaged Nusselt number along the streamwise direction, Nu_x, for the plain fin and slit fin surfaces, where x is the streamwise coordinate starting from the very beginning of the full computational domain with length unit of meter. Noting that

two types of fin have the same depth in the airflow direction. Generally speaking, the values of Nu_x of the plain fin decrease along the streamwise direction. The values of Nu_x of the slit fin, however, change up-and-down streamwisely, and many local peaks appear over the entire fin region. It is interesting to note that roughly speaking each peaks corresponds to each strip: in the leading edge of a strip the local heat transfer increase, while it decreases abruptly behind the strip. Big difference between the local Nusselt numbers of the slit fin and plain plate fin can be clearly observed. From the traditional point of view the gradual streamwise decrease of the local Nusselt number of the plain plate fin can be explained by the streamwise increase in the thermal boundary layer thickness, and the up-and-down variation of the local heat transfer of the slit fin can be attributed to the increasing interruption in the fluid. As demonstrated in Tao et al. (2002a), all these explains can be unified by the FSP. This will be illustrated in the following section.

Figure 13 Variation of Nu_x for the plain plate fin and slit fin

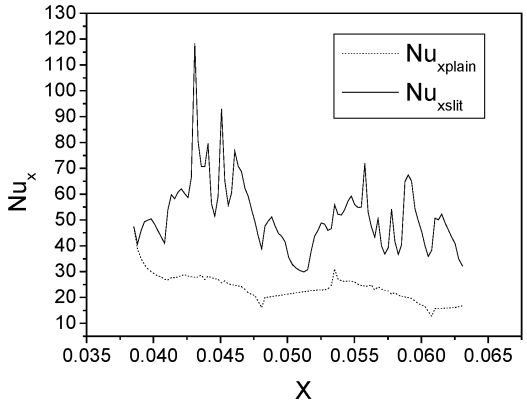

4.4 Analysis from Field Synergy Principle (FSP)

The problem at hand is a 3-D situation. However, as can be expected from Figures 4 and 5, the velocity components in z-direction are much smaller than that in x- and y-directions because of the space limitation. For the simplicity of computation, we take the mid plane between two adjacent fin sheets into consideration. That is, we take the velocity distribution and temperature contours in the plane of $z = p_f/2$ as the representative of the entire domain. Our experiences have shown that this will lead to some quantitative difference, but will not affect the qualitative conclusion. In Figure 14, temperature contours at the middle plane for two types of fins with u_{in} = 2.0 m/s are presented. Following features may be noted. First, at the flow inlet region of the two fins, the temperature isothermals are mostly parallel to the inlet boundary. Second, there exist two regions behind the two cylinders where the fluid isotherms almost go along with the flow direction. Third, for the slit fin in the downstream part, the regions with streamwise isotherms are significantly reduced, and there exist many isotherms, which go spanwisely. By combination with the flow fields, these characteristics of the isotherm distributions can well reveal the essence of why slit fin can enhance heat transfer. To proceed, the streamwise lines are supplemented in the fluid isotherms and the resulting pictures are provided in Figure 15 where the streamwise lines are equipped with arrows. It can be clearly observed following facts: First in the inlet regions of the two fins, the velocity is almost perpendicular to the fluid isothermal, indicating a good synergy between the local velocity and temperature gradient; Second, in the downstream part of the plain plate fin, except a narrow region in the middle part where the local streamline is almost perpendicular to the isotherm, there is a quite large region where the streamlines are almost parallel to the isotherms, implying a bad synergy between velocity and temperature gradient. Third, for the slit fin, there is a rather large area in the downstream part where the local streamline is almost perpendicular to the isothermals, which means that the synergy in the downstream part is improved.

Figure 14 Temperature contours at middle plane $z = P_f/2$ for two types of fin: (a) plain plate fin and (b) radially slit fin

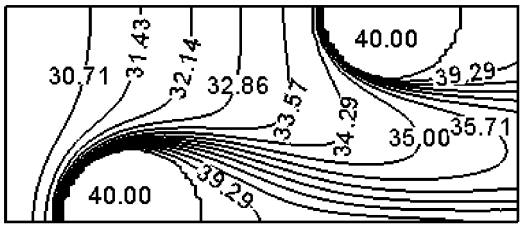

(a)

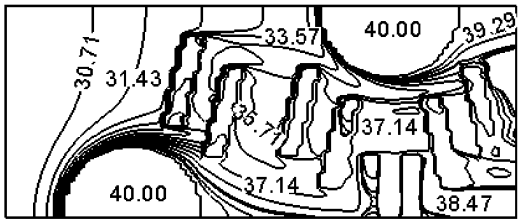

(b)

Figure 15 Streamline and isotherm patterns at middle plane $z = P_f/2$ for two types of fin: (a) plain plate fin and (b) radially slit fin

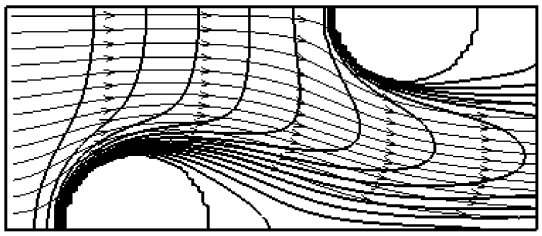

(a)

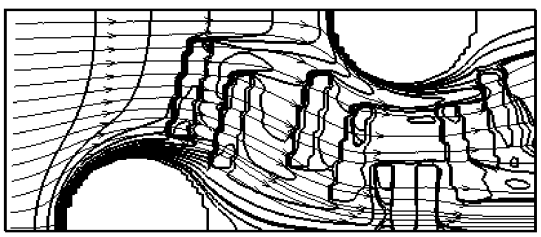

(b)

Finally, the streamwise synergy angle distribution is presented. In Figure 16, the variations of the spanwise averaged synergy angle, θ_x, along the streamwise direction for the plain plate fin surface is shown. It can be clearly observed that with the increase in streamwise coordinate, the local heat transfer coefficient decreases and the spanwise average synergy angle increases, which is fully consistent with the analysis made above: where the local heat transfer is enhanced, there is a reduced synergy angle. The streamwise local distribution of the synergy angle for the slit fin is presented in Figure 17, where the same variation trend can be observed. The domain average synergy angle of the plain plat fin and the slit fin are 88.3° and 87°, respectively. It should be noted that in the range of an angle close to 90°, a slight change in angle leads to a big variation in its cosine function. The ratio of the cosine functions corresponding to the above two angles is about 0.58. Here the absolute value may not make sense, but does quantitatively indicate which one has a better heat transfer performance.

Figure 16 Variation of θ_x for the plain plate fin surface

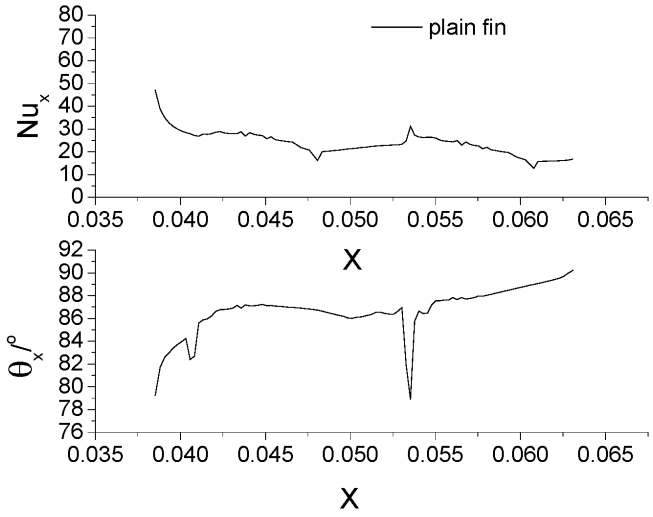

Figure 17 Variation of θ_x for the slit fin surface

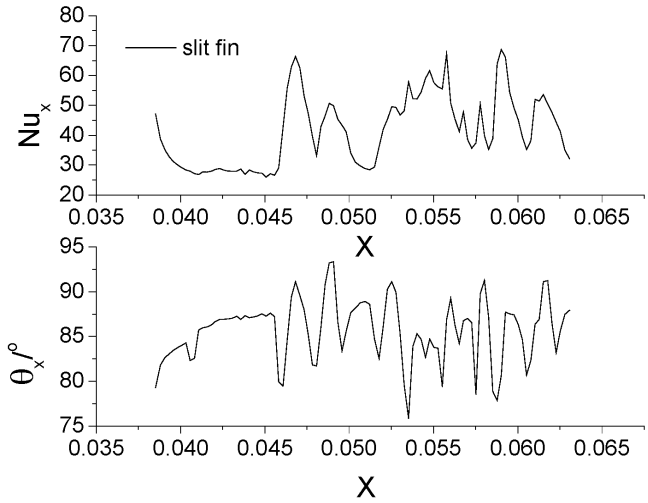

5 Conclusions

In this paper, the air fluid flow and heat transfer characteristics of a radially slotted fin surface of a two-row heat exchanger and comparison with its counterpart of a plain plate fin are numerically studied. The major conclusions are as follows.

- Numerical results show that both heat transfer rate and pressure drop of the two kinds of surfaces increase with the frontal velocity. At the same frontal velocity heat transfer rate of the slotted fin surface is higher than that of plain plate fin surface, meanwhile, the pressure drop of the slotted fin surface is also appreciably higher than that of the plain one.
- It is found that at the identical pumping power or the identical pressure drop, the performance of the slotted fin surface studied is much better than that of the plain fin surface. Under the identical pressure drop constraint, the radially slotted fin surface may provide 10–30% enhancement in heat transfer, and under the identical pumping power condition, it offers 20–40% enhancement.
- It is found that the average intersection angle of the slotted fin surface is less than that of the plain plate fin surface at the same frontal velocity, showing the feasibility of the FSP in analysing the enhancement of heat transfer.

Acknowledgement

This work was supported by the National Natural Science Foundation of China (No. 50476046) and the Research Foundation of Doctorial Project (RFDP20030698015).

References

Atkinson, K.N., Drakulic, R. and Cowell, A. (1998) 'Two- and three-dimensional numerical models of flow and heat transfer over louvered fin arrays in compact heat exchangers', *Int. J. Heat Mass Transfer*, Vol. 41, No. 24, pp.4063–4080.

Cheng, Y.P., Qu, Z.G., Tao, W.Q. and He, Y.L. (2004) 'Numerical design of efficient slotted fin surface based on the field synergy principle', *Numerical Heat Transfer: Part A: Applications*, Vol. 45, No. 6, pp.517–538.

Comini, G. and Groce, G. (2001) 'Convective heat mass transfer in tube-fin exchangers under dehumidifying conditions', *Numerical Heat Transfer. Part A*, Vol. 40, No. 6, pp.579–599.

Guo, Z.Y., Li, D.Y. and Wang, B.X. (1998) 'A novel concept for convective heat transfer enhancement', *Int. J. Heat Mass Transfer*, Vol. 41, No. 14, pp.2221–2225.

He, Y.L., Tao, W.Q., Song, F.Q. and Zhang, W. (2005) 'Three-dimensional numerical study of heat transfer characteristics of plain plate fin-and-tube heat exchanger from viewpoint of field synergy principle', *Int. J. Heat Fluid Flow*, Vol. 6, No. 3, pp.459–473.

Jacobi, A.M. and Shah, R.K. (1998) 'Air-side flow and heat transfer in compact heat exchangers: a discussion of enhancement mechanism', *Heat Transfer Engineering*, Vol. 19, No. 4, pp.29–41.

Kang, H.J., Li, W., Li, H.J., Xin, R.C. and Tao, W.Q. (1994) 'Experiment study on heat transfer and pressure drop characteristics of four types of plate fin-and-tube heat exchanger surfaces', *J. Thermal Science*, Vol. 3, No. 1, pp.34–42.

Leu, J.S., Liu, M.S., Liaw, J.S. and Wang, C.C. (2001) 'A numerical investigation of louvered fin-and-tube heat exchangers having circular and oval tube configuration', *Int. J. Heat Mass Transfer*, Vol. 44, No. 22, pp.4235–4243.

Min, J.C. and Web, R.L. (2001) 'Numerical predictions of wavy fin coil performance', *Journal of Enhanced Heat Transfer*, Vol. 8, No. 3, pp.159–173.

Patankar, S.V. (1980) *Numerical Heat Transfer and Fluid Flow*, McGraw-Hill, New York.

Qu, Z.G., Tao, W.Q. and He, Y.L. (2004) 'Three-dimensional numerical simulation of laminar heat transfer and fluid flow characteristics of strip fin surface with X-arrangements of strips', *Journal of Heat Transfer*, Vol. 126, No. 5, pp.697–707.

Shah, R.K. and Sekulic, D.P. (2003) *Fundamentals of Heat Exchanger Design*, John Wiley & Sons, New York, p.941.

Tao, W-Q., Guo, Z-Y. and Wang, B-X. (2002a) 'Field synergy principle for enhancing convective heat transfer – its extension and numerical verifications', *International Journal of Heat and Mass Transfer*, Vol. 45, No. 18, pp.3849–3856.

Tao, W.Q., He, Y.L., Wang, Q.W., Qu, Z.G. and Song, F.Q. (2002b) 'A unified analysis on enhancing single phase convective heat transfer with field synergy principle', *International Journal of Heat and Mass Transfer*, Vol. 45, No. 24, pp.4871–4879.

Webb, R.L. (1994) *Principle of Enhanced Heat Transfer*, John Wiley & Sons, Inc. New York, p.556.

Yun, J.Y. and Lee, K.L. (2000) 'Influence of design parameters on the heat transfer and flow friction characteristics of the heat exchanger with slit fins', *Int. J. Heat Mass Transfer*, Vol. 43, No. 14, pp.2529–2539.

Nomenclature

α	Included acute angle between radial slit and x coordinate, °
A	Area, mm^2
c_p	Specific heat capacity at constant pressure, $Jkg^{-1}k^{-1}$
d	Outer tube diameter, mm
f	Friction factor
L	Heat exchanger depth in air flow direction, mm
Nu	Nusselt number
NuF	The goodness factor of a design
$NuF_{1/2}$	The goodness factor of a design
$NuF_{1/3}$	The goodness factor of a design
p_f	Fin pitch, mm
P	Pressure, Pa
Pr	Prandtl number
ΔP	Pressure drop, Pa
Q	Heat transfer rate, J
Re	Reynolds number
∇T	Temperature gradient, °C/m
ΔT_{lg}	The logarithmic mean temperature difference, °C
T	Temperature, °C
u	Velocity component along x coordinate, m/s
v	Velocity component along y coordinate, m/s
w	Velocity component along z coordinate, m/s
x,y,z	Cartesian coordinates, m
Greek symbols	
Γ	Diffusion coefficient, m^2/s
θ	Intersection angle between velocity and temperature gradient (°)
λ	Thermal conductivity, W/(m.K)
v	Kinematic viscosity, kg/(m.s)
ρ	Air density, kgm^{-3}
ϕ	General variable
Subscripts and superscripts	
0	Reference value
b	Bulk
en	Enhanced
in	Inlet
lg	Logarithmic
max	Maximum
min	Minimum
out	Outlet
p	Pressure
x	Local position